ADVANCED FUNCTIONAL MATERIALS
www.afm-journal.de

A Single Integrated 3D-Printing Process Customizes Elastic and Sustainable Triboelectric Nanogenerators for Wearable Electronics

*Shuo Chen, Tao Huang, Han Zuo, Sihao Qian, Yifan Guo, Lijie Sun, Dong Lei, Qilin Wu, Bo Zhu, Chuanglong He, Xiumei Mo, Eric Jeffries, Hao Yu, and Zhengwei You**

Triboelectric nanogenerator (TENG) devices have gotten great attention in wearable power sources and physiological monitoring. However, the complicated assembling and the molding processing retard their applications. Here, 3D-printed TENGs (3DP-TENGs) are designed and readily fabricated by a single integrated process without additional assembling steps. The TENGs contain poly(glycerol sebacate) (PGS) and carbon nanotubes (CNTs) as the two electrification components. Conductive CNTs also serve as electrodes. Elastic PGS matrix makes TENGs intrinsically responsive to biomechanical motions leading to robust energy outputs. The hierarchical porous structure of the 3DP-TENG results in higher output efficiency than traditional molded microporous TENG counterparts. TENGs with different 3D shapes are readily fabricated for different applications. The 3DP-TENG insole efficiently harvests biomechanical energy to drive electronics. A ring-shaped TENG acts as a self-powered sensor to monitor the motion of fingers. Furthermore, the use of bio-based and biodegradable PGS matrix combining with efficient recycle of CNTs makes 3DP-TENGs favorable from sustainable perspective. This work provides a new strategy to design and tailor 3D TENGs that will be very useful for diverse electronic applications.

1. Introduction

Recently, triboelectric nanogenerators (TENGs), first reported by Wang's group, which generate electricity by triboelectrification and electrostatic induction, have emerged as a new paradigm for harvesting mechanical energy from human body motions and monitoring physiological activities.[1] Thanks to flexible structure design, varied material selection, and green energy generation, TENGs have achieved rapid progress in both academia and industry.[2] However, previous reported TENGs are generally composed of multiple independent layers such as two triboelectric components and their corresponding electrodes.[3] The complex structures and thus sequential assembly steps make it challenging to achieve scalable 3D fabrication and strechability, which is highly desired for emerging wearable electronic devices.[4] Recently, several TENGs based on integrating conducting materials and elastomeric substrates without additional assembling process have been developed.[2c,4,5] In view of the fact that these TENGs are typically fabricated by molding, it is hard to make 3D sophisticated shapes for practical applications. Nowadays, 3D-printing has been recognized as a revolutionary manufacturing technology and received significant attentions from both industry and society. This computer-aided additive manufacturing technology can readily customize complex 3D geometries with well-controlled micro- and macrostructure from diverse materials. Due to its clear advantages, 3D-printing has been widely used in the manufacturing of a variety of electronic and biomedical devices.[8] Lately, Chen et al. reported first 3D-printed ultraflexible TENG.[6] However, the TENG has an intricate architecture, consisting of two triboelectric resin parts and lots of cylinder-shaped ionic hydrogel electrodes. As a result, a complicated, multiple-step process is needed to fabricate such a TENG.

TENGs aim to harvest abundant clean and renewable energy all over the world including human motion, flowing water, and wind to generate electricity for diverse applications, thus, are very attractive from sustainability perspective. Compared to extensive research to enhance power generation of TENGs,

S. Chen, T. Huang, H. Zuo, S. Qian, Y. Guo, L. Sun, D. Lei, Prof. Q. Wu, Prof. H. Yu, Prof. Z. You
State Key Laboratory for Modification of Chemical Fibers and Polymer Materials
College of Materials Science and Engineering
Donghua University
Shanghai 201620, China
E-mail: zyou@dhu.edu.cn
Prof. B. Zhu
School of Materials Science and Engineering
Shanghai University
Shanghai 200444, China
Prof. C. He, Prof. X. Mo
College of Chemistry
Chemical Engineering and Biotechnology
Donghua University
Shanghai 201620, China
Dr. E. Jeffries
6120 Fillmore Place, Apt 2, West New York, NJ 07093, USA
The ORCID identification number(s) for the author(s) of this article can be found under https://doi.org/10.1002/adfm.201805108.

DOI: 10.1002/adfm.201805108

less attention has paid on the sustainability of the materials used. Most reported TENGs are made from nondegradable, nonrenewable petro-based materials, which will significantly compromise the overall sustainability of TENGs. Recently, a few biodegradable synthetic polymers and natural biopolymers have shown promising to make TENGs.[7] However, more sustainable materials are highly desired to fully realize the potential of TENGs as renewable energy harvesters.

To address the aforementioned challenges in TENGs, we develop a simple, scalable, and versatile strategy to fabricate bio-based, biodegradable, integrated and elastic 3D-printed TENGs (3DP-TENGs). The 3DP-TENG with single electrode mode structure made from only two materials, poly(glycerol sebacate) (PGS) and carbon nanotubes (CNTs), thus, can be readily fabricated in one-step direct ink writing (DIW) process without further assembling procedure. The resultant 3DP-TENG has a hierarchical porous structure, which is hardly achieved through traditional molding method.[8] Each individual pore is a small TENG unit, where PGS matrix and composited CNTs serve as the two triboelectric components. At the same time, CNTs construct a connected conductive network used as electrodes. When applied with mechanical force, the electrification between the exposed CNTs and the PGS matrix on the surface of the deformed pores induces the flow electrons between the CNTs network and ground.[4] Based on the 3D-printing technologies, the new developed 3DP-TENGs can be processed into variable 3D shapes to meet different requirements, especially useful for wearable electronics demonstrated by an insole-shaped energy harvester and a ring-shaped sensor.

It is worthy to note that we use a biomaterial PGS to build TENGs. PGS made from bio-based sebacic acid and glycerol is an excellent sustainable material with proven biodegradability, biocompatibility and has been widely used in biomedical engineering.[9] Thus, the utilization of PGS to harvest biomechanical energy well accords with the sustainability principle of TENGs. Furthermore, we successfully recycle expensive CNTs based on the biodegradability of PGS matrix and demonstrate their feasibility to refabricate 3DP-TENGs. All these make the 3DP-TENGs especially valuable for ecofriendly and economical electrical applications.

2. Results and Discussion

Schematic diagram of the fabrication of the 3DP-TENGs is shown in **Figure 1**a. The PGS was prepared by polycondensation of an equimolar mixture of glycerol and sebacate. The structure of PGS was characterized by NMR and Fourier transform infrared spectroscopy (Figure S1, Supporting Information). CNTs and salt particles were added to the PGS to prepare the extrudable printing ink. The paste-like composited ink could be solidified rapidly after extrusion to obtain designed 3D structures (Figure S2, Supporting Information), which were further thermo-cured to deliver robust and elastic 3DP-TENGs. It should be noted that the 3D-printing of the thermoset PGS elastomer still remains a challenge due to its poor shape-retention during high temperature curing. We addressed this issue by compositing the salt particles and CNTs with PGS. The salt particles and CNTs used here not only serve as sacrificial template and conductive materials but also play a role as reinforce fillers in the composited inks. Due to the interface interaction between the fillers and matrix, the composited inks could keep the 3D printing structure at high temperature. The weight ratio of PGS and salt particles was optimized to be 1:1.25, with a 10 wt% CNTs content. Lower salt ratio could not efficiently support the 3D structures, while composite ink with higher salt ratio could not be printed continuously. We further evaluated the printability of composited inks with different CNTs contents. For better electrical output performance, higher weight ratios of CNTs (15 and 20 wt%) were investigated. The composited inks with 15 wt% CNTs could be extruded smoothly and maintain the extruded 3D structures. The composited ink with 20 wt% CNTs showed poor extrudability even at 100 °C because of the higher viscosity (Figure S3, Supporting Information). Therefore, composited inks with 10 and 15 wt% CNTs were used for further experiments. Efficient printing of multiple 3D TENGs with different sizes and architectures demonstrated the flexibility and scalability of our method (Figure 1b). This will be very useful to fabricate sophisticated geometries to fit various actual applications.

The combination of DIW and salt particles enables the design of the hierarchical porous structures at the millimeter and micrometer scales. This complex multiporous architecture of the 3DP-TENGs is hardly achieved through traditional molding process. The scanning electron microscopy (SEM) images show the hierarchical porous structure (Figure 1c). The mm-sized open pores in the lattice architectures could be controlled by adjusting the distance between printing filaments (Figure 1c,i). Extensive pores in sizes of tens micrometers generated by salt leaching distributed in the filaments (Figure 1c,ii,iii). Exposed CNTs on the surface of pores evidenced by SEM image (Figure 1c,iv, red arrows) made the electricity-generation process possible. The elastic crosslinked PGS matrix and the designed hierarchical porous structure make the 3DP-TENGs elastic and resistant to different mechanical deformations (Figure S4, Supporting Information). The elasticity of the prepared 3DP-TENGs was evaluated by cyclic compression test. Negligible hysteresis after 100 cycles according to the strain–stress curves revealed the excellent elasticity of the 3DP-TENG (Figure 1d), which was very important for reliable electric output performance. The mechanical properties of the 3DP-TENG with different CNTs contents were evaluated with a uniaxial compression test (Figure S5, Supporting Information). The compression strength at a strain of 40% and modulus of the 3DP-TENG increased with the increase of CNTs contents likely due to the toughening effect of the CNTs composited in the PGS matrix. The compressive modulus of the 3DP-TENG with 15 wt% CNTs content was 430 ± 60 kPa comparable to the mechanical properties of native soft tissues such as muscles.[10] Accordingly, these 3DP-TENGs could easily be deformed by biomechanical motion due to their relatively low moduli.

As shown in **Figure 2**a, the electricity-generation process of the 3DP-TENGs is based on compressive deformation and can be described as the single-electrode TENGs. CNTs distributed all over the PGS matrix to form a conductive network. The CNTs on the surface of the pores of 3DP-TENG were partially imbedded in PGS. When the pore was compressed, exposed parts of CNTs on the wall touched with the PGS matrix in

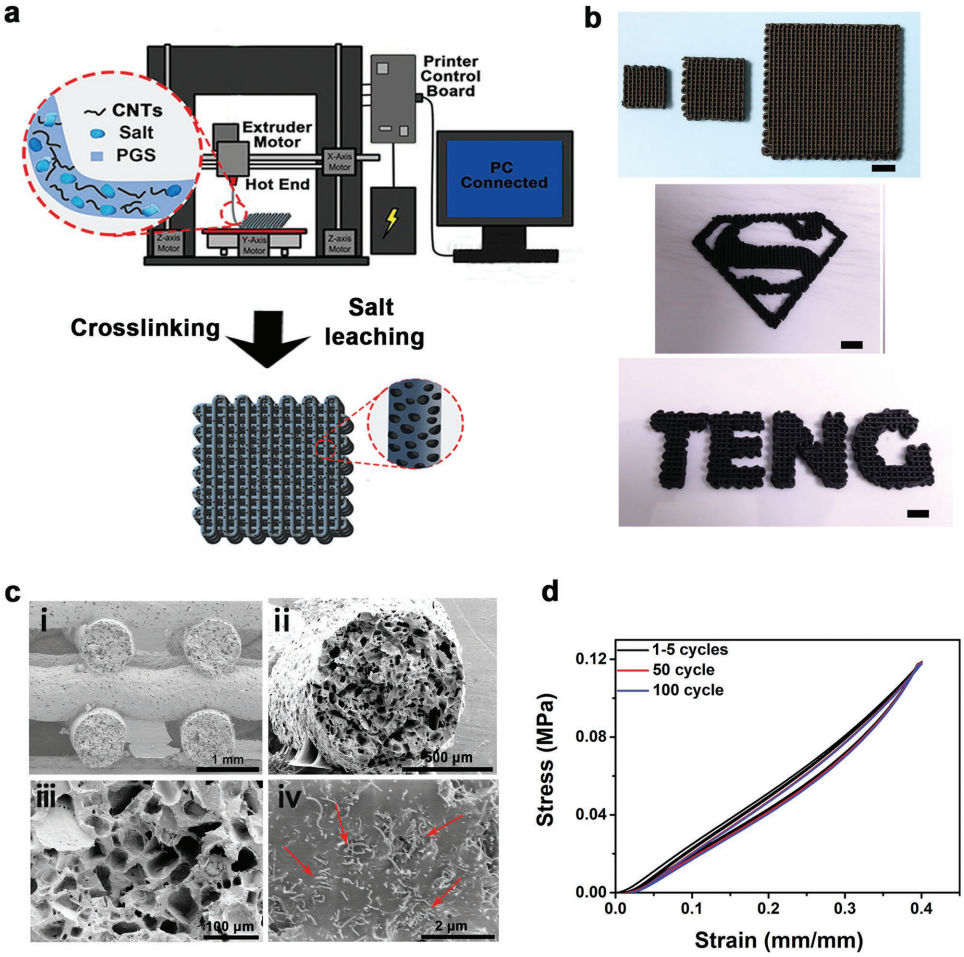

Figure 1. The fabrication and properties of the 3DP-TENGs. a) Schematic diagram of the fabrication of the 3DP-TENGs and the hierarchical porous structure. b) Photographs of 3DP-TENGs with diverse morphologies: cubic lattices with different sizes (top), a "superman" logo (middle), and a "TENG" logo (bottom), scale bar = 10 mm. c) The SEM images of mm-sized open pores built by i) the aligned microfilaments, ii) the cross-section of a single microfilament, iii) the random distributed micropores in the filaments, and iv) the inner surface of a single micropore with the exposed CNTs (red arrow). d) The strain–stress curves of cyclic compression test of 3DP-TENG with 15 wt% CNTs content show its excellent elasticity.

another side and became positively charged due to their weaker ability to capture negative charges than PGS. PGS gained the electrons and became negatively charged. When the force was unloaded, the elastic squeezed pore would recover its original morphology. Once the PGS matrix separated from the CNTs, the positive charges on the CNTs would increase the electric potential. Since the CNTs grounded, induced electrons flowed from ground to the CNTs network to balance the potential. Furthermore, CNTs network might have residual induced positive charges due to the electrostatic induction effect. When the pore was compressed again, the electrons gathering in PGS matrix flowed back to ground, resulting in an instantaneous current in the opposite direction. Due to the conductive CNTs network, a large amount of pores in different size scales were connected. They deformed and recovered simultaneously according to the external loads, leading to a cumulative electrical output from individual pores.

We printed 3DP-TENG with 15 wt% CNTs in a size of 3 cm × 3 cm × 0.5 cm (length × width × height) to measure the electrical output. During the electrical measurement, a force was periodically loaded onto the 3DP-TENG to yield a compressive strain of 40% at a frequency of 3 Hz (Figure S6, Supporting Information). The peak voltage was 45 V at open-circuit conditions (Figure 2b). Under short-circuit conditions, the volume current density reached a peak value of 190 mA m^{-3} (Figure 2c), higher than previous reported 3D printed TENG.[6] Furthermore, the 3DP-TENG could reach a maximum instantaneous power density of 1.11 W m^{-3} at an external load resistance of 50 MΩ (Figure S7, Supporting Information). The long-term stability/reliability of the 3DP-TENG was also examined (**Figure 3**d). The 3DP-TENG withstood more than 6000 cycles of deformations at a compression strain of 40% and a frequency of 3 Hz. The gradual accumulation of triboelectric charge even led to increased voltages, consistent with a previous report.[4] The output performance of the 3DP-TENG highly dependent on the compression strain and the contact frequency. The compression strains of each cycle were controlled by a programmed mechanical motor. The output voltages of the 3DP-TENGs linearly increased with the compressing strains and reached a peak output voltage of 71 V at a 70% compression strain (Figure 2e)

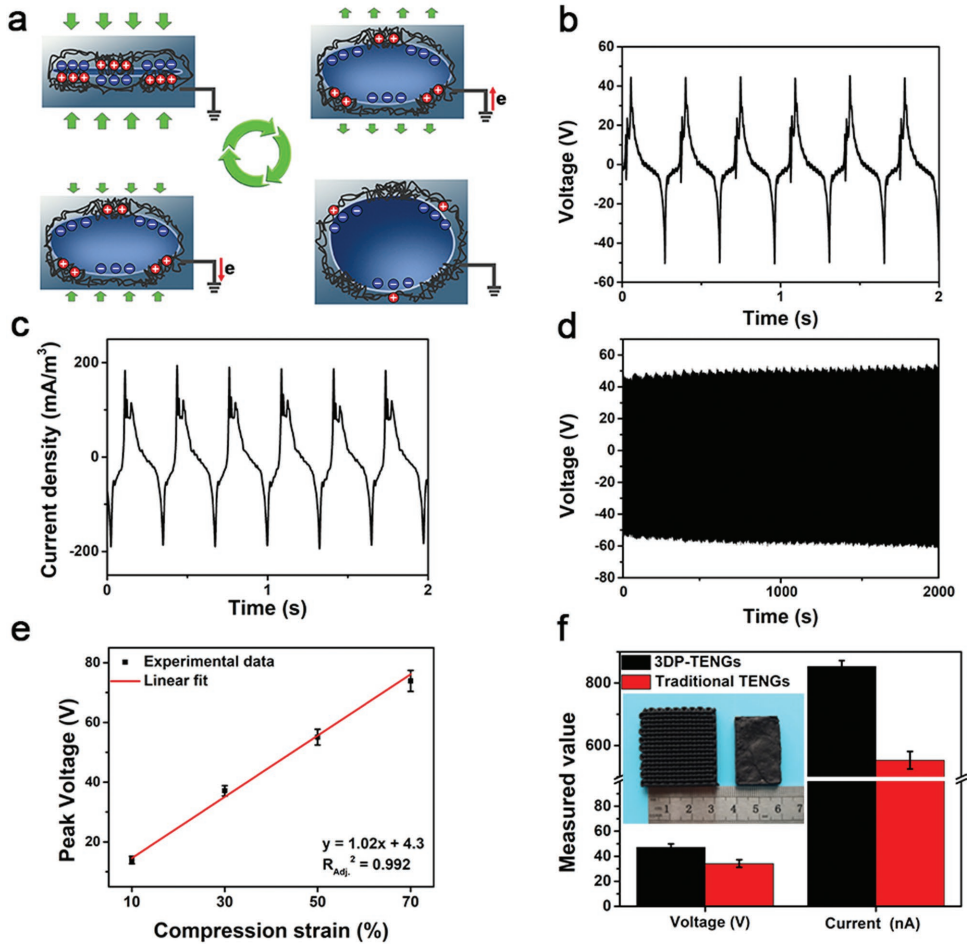

Figure 2. Electricity generation principle and electrical characterization of 3DP-TENGs. a) Schematic diagram showing the working principles of a single pore. b,c) The corresponding output voltage and current density of 3DP-TENGs with a cyclic compressive strain of 40%. d) The durability test of 3DP-TENGs. The output voltage was monitored for 6000 cycles with a compressive strain of 40%. e) Linear dependence of the peak output voltage on different compression strains. f) The comparison of output performance of the hierarchical porous 3DP-TENGs and the counterpart microporous TNEGs fabricated by traditional molding method, both of which were made from the same amount of composite ink.

because the higher compression ratio increased the contact area inside the deformed pores and consequently increased triboelectric charges per unit volume. The output voltage increased from 15 to 76 V when the contact frequency rose from 1 to 4 Hz (Figure S8, Supporting Information). The increased voltage was attributed to the enhanced induction and transferring of charges under higher frequency contact. As designed, the CNTs content also affected the electrical output. The electrical output voltage of the 3DP-TENGs with 15 wt% CNTs was higher than the ones with 10 wt% CNTs (Figure S9, Supporting Information). There were two main reasons for this phenomenon. First, the higher CNTs content led to more exposed CNTs for enhanced triboelectrification (Figure S10, Supporting Information). Second, the resistivity (four-probe measurement) significantly decreased by more than two orders of magnitude, from 41 MΩ m at 10 wt% to 0.43 MΩ m at 15 wt% (Figure S11, Supporting Information).

The output efficiency of hierarchical porous 3DP-TENGs was compared with the microporous TNEGs with same compositions fabricated by solution casting in molds. As shown in Figure 2f, the output voltage and current of the 3DP-TENG were both higher than the microporous TENG, indicating that the superior output electrical performance of the 3DP-TENG. It should be emphasized that the 3DP-TENG and microporous TENG were made from a same amount of composited inks (Figure S12, Supporting Information). The size of the 3DP-TENG was almost 1.5 times larger than the microporous TENG (inset of the Figure 2f) with the same thickness, indicating more porous structures in 3DP-TENG. Considering the same amount of microsized salt particles was used as template, the quantity of electric charges generated from the inner surfaces of the μm-sized pores was theoretically equal for these two different TENGs. However, for 3DP-TENG, there were lots of mm-sized open pores between the filaments. When the 3DP-TENGs were stimulated by external force, the mm-sized pores deformed and recovered simultaneously, serving as additional electricity generation units (Figure S13, Supporting Information). The increased contact surface area from the mm-sized pores was the key for the superior output efficiency of 3DP-TENG. These results revealed that the hierarchical porous structures in TENGs alone played an important role in output electrical performance without adjusting the materials. In

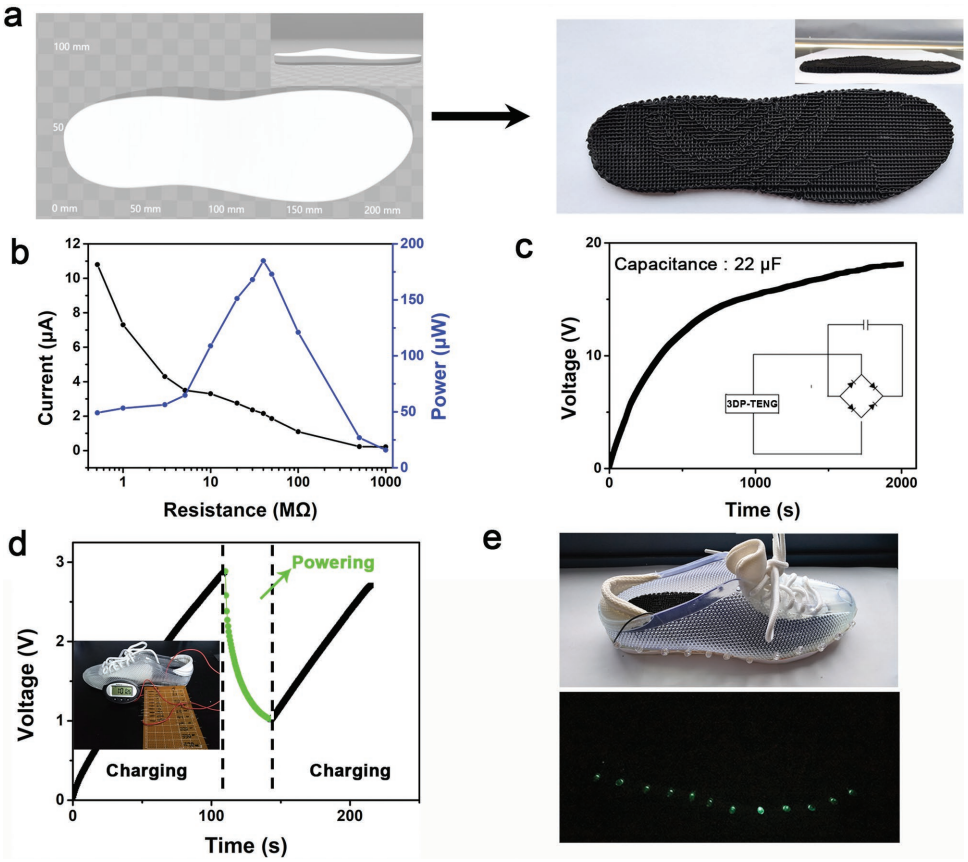

Figure 3. Energy harvesting of a 3DP-TENG insole. a) The images of top view and side view (insets) of a digital model (left) and corresponding 3DP-TENG insole (right). b) Output currents and powers of the 3DP-TENG insole under various external loads. c) Charging curve of a commercial capacitor (22 μF) by the 3DP-TENG insole. d) Voltage profile of a 22 μF capacitor being charged by the 3DP-TENG insole and powering the electronic watch. Image of the self-charging system to power electronic watch (inset). e) Photograph of a self-powered lighting shoe with a 3DP-TENG insole inside (top) and the simultaneously lighting LEDs while the wearer stomped (bottom).

view of the strong design freedom of 3D-printing method, it is expected to fabricate 3DP-TENGs with more effective multi-porosity features for high performance in future.

The TENGs used as insoles have been proven an effective way to harvest biomechanical energy.[1c,e,6,11] Prior work has achieved good results on the flexibility, output performance, and stability. However, the previous reported TENGs used as insoles are generally fabricated by assembling different parts together to obtain elastic 3D structures.[1c,6] The complex manufacturing process makes the production challenging. Recently, 3D-printed insoles have drawn an increasing attention and have been commercialized due to their customized features and excellent comfortableness. Our newly developed 3D-printing TENG technology is quite simple and can be well integrated with 3D-printing insole process for practical applications. The precise controllable 3D-printing technology could fabricate the designed shapes to conform the curvilinear surface of the foot and might yield improved comfort comparable to previously reported TENGs insoles. Accordingly, we fabricated the 3DP-TENG insoles and evaluated their ability to harvest biomechanical energy. The digital model of the insole was made via the Solidwork software and used as stereolithographic format. The 3D printing process followed the pathways generated from the corresponding digital model to get the final 3D printed insole (**Figure 4**a). A 55 kg volunteer stomped with the insole continuously with a frequency of ≈1.5 Hz to generate electricity. The peak voltage produced by the 3D-TENG insole was about 170 V (Figure S1, Supporting Information). Figure 4b shows output currents and maximum output powers measured under external loads of 0.51–1000 MΩ. The output power was determined by the following equation: $P_i = U_i^2/R$. where P_i, U_i, and R were the instantaneous power, the peak voltage, and the external load of the 3DP-TENG insole, respectively. With the increase of the external loads, the output current showed a downward trend due to the limited charge flow. As a result, the 3DP-TENG insole reached a maximum instantaneous power of 185.2 μW at an external load resistance of 40 MΩ. To evaluate the potential of the 3DP-TENG insole as a power source, the capacitor charging characteristics of the 3DP-TENG insole was investigated (Figure 3b). A rectifier was integrated in series with the 3DP-TENG insole. A commercial capacitor of 22 μF was serially connected to above circuit as electrical energy storage (the inset of Figure 3c). After nearly 4000 working cycles in 2000 s of the 3DP-TENG insole, the capacitor was charged up to 18 V, comparable with previously reported 3D printing TENGs.[6] To further demonstrate charging capability of the 3DP-TENG insole as a practical power source, a self-charging system to power the electronic watch was developed

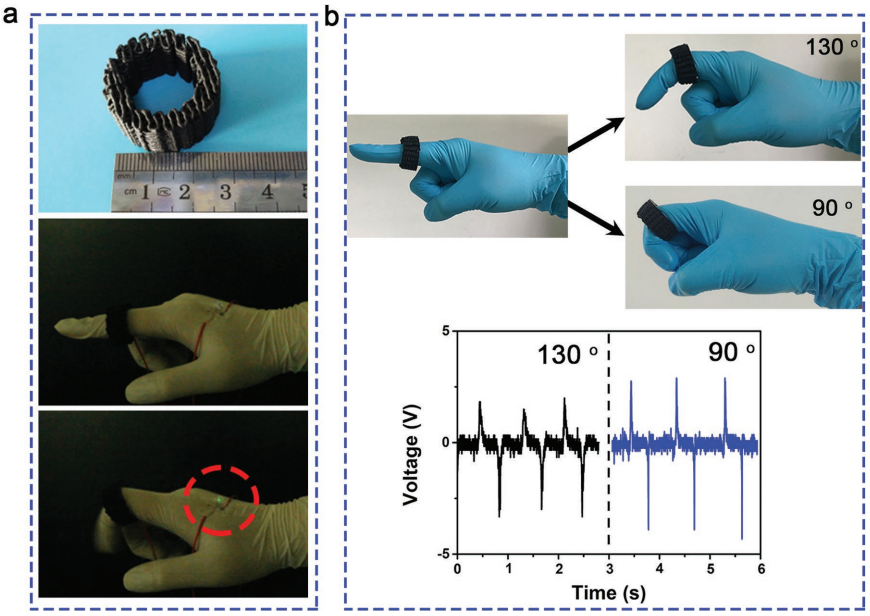

Figure 4. Monitoring of the motions of fingers by a ring-shaped 3DP-TENG. a) Photographs of 3DP-TENG and its monitoring of the finger bending by lighting a green LED. b) The different output voltage profiles of the 3DP-TENG during cyclic finger bending at different angles.

(inset of Figure 3d). The voltage of capacitor increased linearly to the value of 2.8 V in 110 s (Figure 3d and Movie S1, Supporting Information). The self-charging system later powered the electronic watch for about 27 s and the voltage of capacitor dropped steadily. Subsequently, the capacitor was charged back to 2.8 V and powered the electronic watch again, indicating the continuous working ability of the self-charging system. Next, we investigated the ability of 3DP-TENG insole as a biomechanical power source to drive portable electronics. Twelve light-emitting diodes (LEDs) were stuck to the outside of shoe with 3DP-TENG insole to make a self-powered lighting shoe (Figure 3e). The LEDs were simultaneously lit when the wearer stomped on ground (Movie S2, Supporting Information). The intermittent LEDs light could be used as the warning signs for the night running. The 3DP-TENG insole showed great potential to harvest biomechanical energy to build sustainable self-powered electronic systems. Due to the flexibility of 3D printing, this technology can readily fabricate shape-adaptable TENGs to fit the irregular geometries of different applications especially useful for portable and wearable power sources.

The output signals of the 3DP-TENGs induced from mechanical motion can also be used as a self-powered mechanical sensor. Real-time and continuous human motion monitoring could provide bio-feedbacks for physiological evaluation and rehabilitation.[12] As an exemplification, a ring-shaped 3DP-TENG was fabricated to monitor the motions of fingers (Figure 4a and Movie S3, Supporting Information). The ring-shaped 3DP-TENG was worn on a finger joint. Cyclic finger bending was efficiently monitored by synchronous blinking of a connected green LED. We further evaluated a ring-shaped 3DP-TENG for monitoring the bending angles of figures by measuring the output voltages (Figure 4b). The smaller bending angle (90°) of the finger corresponding to the larger deformation of the 3DP-TENG generated higher output peak voltage compared to the larger bending angle (130°). It was consistent with our previous result (Figure 2e). Accordingly, this ring-shaped sensor can be further used to monitor the hand gestures for smart applications such as robots, remote controllers, and Internet of Things. It is noteworthy that this hierarchical porous ring-shaped TENG is relatively hard to be fabricated by traditional molding method. Using 3D printing technology, we could tailor more sophisticated 3D constructs to fit diverse demands in various applications.

PGS has been proven to be biodegradable by many researches.[9] The main mechanism of degradation is the cleavage of the ester linkages resulting in glycerol and sebacic acid.[13] Glycerol and sebacic acid both bio-based, existing in native body, and have well documented biocompatibility. Thus, PGS is an excellent sustainable material in full life cycle. From the environmental and economic perspectives, the recycle of CNTs would further improve the sustainability of 3DP-TENGs. Accordingly, we evaluated the enzymatic degradation of PGS matrix, consequent recycle and reuse of CNTs (**Figure 5**a and Figure S15, Supporting Information). First, the 3DP-TENGs were put in a lipase (from thermomyces lanuginosus) solution with a concentration of 2000 U mL^{-1}. As previously reported, PGS matrix underwent a surface erosion degradation with a good retention of geometric and mechanical integration, superior to typical biodegradable polymer with bulky degradation.[14] In our experiment, 3DP-TENGs also retained the overall geometry and exhibited a gradual decrease of electronic output performance at the initial stage of degradation (Figure S16, Supporting Information). With the degradation of PGS, the peak voltage steadily decreased from 44 to 13 V within 7 d of biodegradation. After 45 d immersion in the lipase solution, the PGS matrix of 3DP-TENGs nearly totally degraded leaving the free CNTs (Figure S17, Supporting Information). The CNTs were readily recycled by simple filtration and showed typical morphology (Figure 5b), which was identical with fresh CNTs (Figure S18, Supporting Information). The recycled CNTs could be well dispersed in ethanol by ultrasonication and readily mixed with PGS and salt particles again to prepare composite inks with a good printing ability. The recycled 3DP-TENGs showed a reliable electrical output performance comparable to fresh one (Figure 5c). No statistical significance in output voltage and current density between the fresh and recycled 3DP-TENGs were observed.

3. Conclusion

In summary, we have developed a simple and versatile strategy to fabricate elastic and sustainable TENGs with

readily tailorable sophisticated 3D architecture for effective biomechanical energy harvesting and self-powered physiological monitoring. To the best of our knowledge, this is the first time to fabricate integrated TENGs through single 3D-printing process without additional assembling processes. Due to the high flexibility and controllability of 3D-printing, we can readily tailor the shapes and morphologies of the 3DP-TENGs to fit various applications. Biomechanical energy harvesting insole and ring-shaped self-powered sensors were 3D-printed as examples to demonstrate the potentials of 3DP-TENGs. More interestingly, we revealed that the 3D microscopic architectures played an important role in the electrical performance and produced hierarchical porous 3DP-TENGs with output voltage and current superior to microporous TENG counterparts fabricated by traditional molding method. Furthermore, we selected biodegradable, biocompatible, and bio-based elastomer PGS as the matrix and demonstrated the feasibility to recycle and reuse CNTs. These make 3DP-TENGs favorable from the perspective of sustainable development. In addition, the 3D printing strategy we developed here is general and can be applied on other materials to furnish various TENGs with diverse properties and functionalities. In view of its simplicity, universality, and strong customization ability, this work may pave a new way to make advanced electronics for a wide range of applications including wearable devices, smart robots, Internet of Thing, and precise medical utilizations.

4. Experimental Section

Materials: PGS was prepared by polycondensation of glycerol (99.5%, Sigma-Aldrich) and sebacic acid (99%, Sigma-Aldrich) as previous reported.[14] Briefly, a mixture of equimolar glycerol and sebacate was placed in flask and melted at 135 °C under nitrogen for 24 h before the pressure was reduced to 250 mTorr over 12 h. White waxy solid PGS was obtained after being cooled to room temperature. The salt particles were acquired from Shanghai Chemical Reagent Plant, P. R. China. The multiwalled carbon nanotubes (CNTs) were purchased from J&K Scientific (99.9%, inner diameter: 5–10 nm, outer diameter: 10–20 nm, length: 10–30 µm).

Preparation of Composited Inks: The PGS was first dissolved in ethyl alcohol with a weight ratio of 1:10. Then, different amounts of CNTs were by dispersed in the solution under ultrasonication for 60 min. The weight ratio between the CNTs and the PGS polymers was adjusted to control the printability. Subsequently, salt particles manually sifted by 37–75 µm sieves were added as the sacrificial template. The mixture was dried under ambient atmosphere for 48 h and then dried in a vacuum oven at 60 °C for 24 h to get a black semi-solid composited ink.

Preparation of 3DP-TENG: Printing was carried out using a commercial available pressure controlled direct ink 3D printing system (HTS-300, Fochif Tech.). Mechanical-driven extrusion of inks was heated and controlled with a digital mechanical regulator using micronozzles with 0.80 mm inner diameter. Filament diameters were around 0.85 mm with extrusion speed 0.008 mm s^{-1}, and deposition speed 2.8 mm s^{-1}, which were the optimized parameters. All printing paths were controlled by external personal computer (PC) control system. The lattice structure was produced by alternating layers of parallel printing lines. The lines of adjacent layer were oriented in a perpendicular fashion. The 3D models of "ring" and "insole" were designed using Solidwork software. The printed 3D structures were put in the vacuum oven at 130 °C curing for 24 h. Then, the solidified 3D structures were immersed in water/ethanol (with a volume ratio of 10:0.5) solution, which was replaced three times every 6 h to completely remove the salts.

The Recycle of CNTs: The 3DP-TENGs were put in a lipase (from thermomyces lanuginosus) aqueous solution with a concentration of 2000 U mL^{-1} at 37 °C under static conditions. The lipase solution was replaced every two days. The samples were taken out at predetermined time (1, 3, and 7 d) and dried for output characterization. After 45 d degradation, the PGS matrix was fully degraded. The suspension was filtered to separate the CNTs. The separated CNTs were washed three times with ethanol to remove the residual degradation products. Then, the washed CNTs were dried under vacuum at room temperature to obtain the recycled CNTs.

Characterization: A Hitachi SU8010 field-emission scanning electron microscope was used to investigate the morphologies of the filaments and the CNTs embedded into the PGS matrix. The mechanical properties were investigated by MTS E42 tensile machine. The

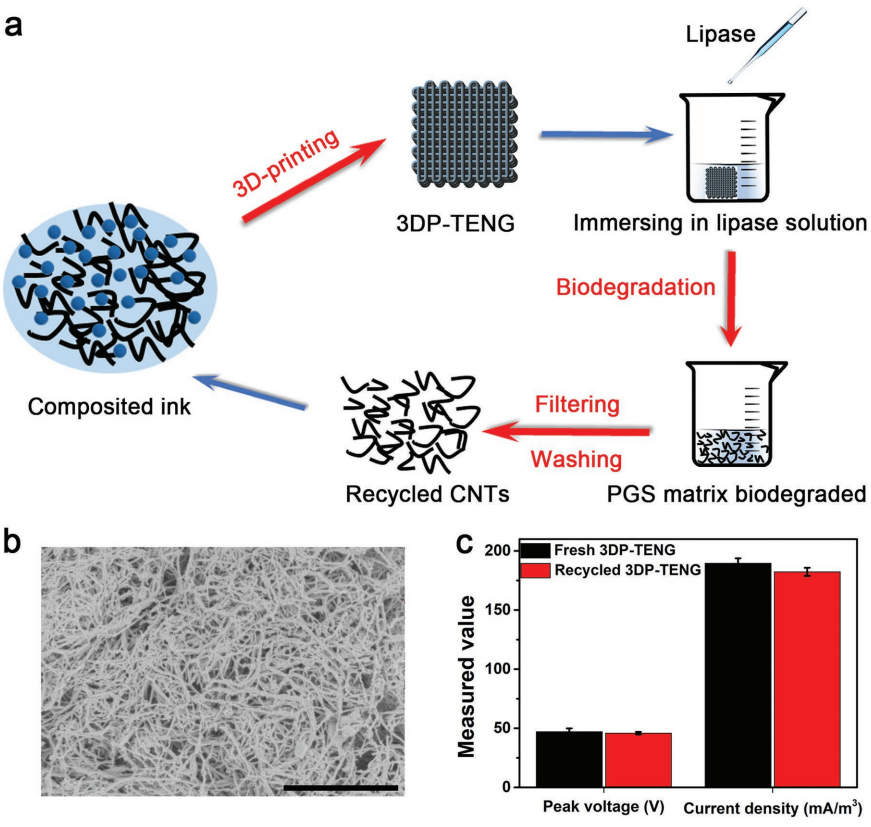

Figure 5. The degradation and recycle of 3DP-TENG. a) Schematic diagram of the degradation and recycling process. b) The SEM image of the recycled CNTs. Scale bar = 2 µm. c) The output performance of the fresh and recycled 3DP-TENGs.

electrical output generated by the 3DP-TENGs (including voltage and current) was measured using a high-power source meter instrument (Model 2657A, Keithley, USA). Measurements were carried out under the force produced by a custom-made apparatus at relative humidity of ≈20% and room temperature.

Supporting Information

Supporting Information is available from the Wiley Online Library or from the author.

Acknowledgements

S.C. and T.H. contributed equally to this work. This work was financially supported by the National Natural Science Foundation of China (21574019, 81320108010, 21474014, and 51703024), the Natural Science Foundation of Shanghai (18ZR1401900), and the Science and Technology Commission of Shanghai (17DZ2260100).

Conflict of Interest

The authors declare no conflict of interest.

Keywords

3D-printing, energy harvesting, hierarchical porous structures, sustainable electronics, triboelectric nanogenerators

Received: July 24, 2018
Revised: August 15, 2018
Published online: September 14, 2018

[1] a) F.-R. Fan, Z.-Q. Tian, Z. L. Wang, *Nano Energy* **2012**, *1*, 328; b) Z. L. Wang, *ACS Nano* **2013**, *7*, 9533; c) J. Wang, S. M. Li, F. Yi, Y. L. Zi, J. Lin, X. F. Wang, Y. L. Xu, Z. L. Wang, *Nat. Commun.* **2016**, *7*, 8; d) Z. Jingdian, Z. Meng, H. Jinrong, B. Jie, J. Yang, W. Magnus, C. Xia, W. Ning, W. Z. Lin, *Adv. Energy Mater.* **2018**, *8*, 1702671; e) S. M. Niu, X. F. Wang, F. Yi, Y. S. Zhou, Z. L. Wang, *Nat. Commun.* **2015**, *6*, 8; f) H. Guo, M.-H. Yeh, Y.-C. Lai, Y. Zi, C. Wu, Z. Wen, C. Hu, Z. L. Wang, *ACS Nano* **2016**, *10*, 10580; g) X. Y. Chen, T. Jiang, Y. Y. Yao, L. Xu, Z. F. Zhao, Z. L. Wang, *Adv. Funct. Mater.* **2016**, *26*, 4906; h) J. Wang, Z. Wen, Y. L. Zi, L. Lin, C. S. Wu, H. Y. Guo, Y. Xi, Y. L. Xu, Z. L. Wang, *Adv. Funct. Mater.* **2016**, *26*, 3542; i) F. Yi, L. Lin, S. M. Niu, P. K. Yang, Z. N. Wang, J. Chen, Y. S. Zhou, Y. L. Zi, J. Wang, Q. L. Liao, Y. Zhang, Z. L. Wang, *Adv. Funct. Mater.* **2015**, *25*, 3688.

[2] a) J. Chen, Y. Huang, N. Zhang, H. Zou, R. Liu, C. Tao, X. Fan, Z. L. Wang, *Nat. Energy* **2016**, *1*, 16138; b) C. Wu, R. Liu, J. Wang, Y. Zi, L. Lin, Z. L. Wang, *Nano Energy* **2017**, *32*, 287; c) Y. C. Lai, J. Deng, S. Niu, W. Peng, C. Wu, R. Liu, Z. Wen, Z. L. Wang, *Adv. Mater.* **2016**, *28*, 10024; d) R. Liu, X. Kuang, J. Deng, Y. C. Wang, A. C. Wang, W. Ding, Y. C. Lai, J. Chen, P. Wang, Z. Lin, *Adv. Mater.* **2018**, *22*, 1705195; e) C. Bo, Y. Ya, W. Z. Lin, *Adv. Energy Mater.* **2018**, *8*, 1702649; f) S. Cheon, H. Kang, H. Kim, Y. Son, J. Y. Lee, H. J. Shin, S. W. Kim, J. H. Cho, *Adv. Funct. Mater.* **2018**, *28*, 7; g) Z. M. Lin, J. Yang, X. S. Li, Y. F. Wu, W. Wei, J. Liu, J. Chen, J. Yang, *Adv. Funct. Mater.* **2018**, *28*, 7; h) C. H. Yao, X. Yin, Y. H. Yu, Z. Y. Cai, X. D. Wang, *Adv. Funct. Mater.* **2017**, *27*, 7.

[3] J. Chun, J. W. Kim, W. S. Jung, C. Y. Kang, S. W. Kim, Z. L. Wang, J. M. Baik, *Energy Environ. Sci.* **2015**, *8*, 3006.

[4] Y. J. Fan, X. S. Meng, H. Y. Li, S. Y. Kuang, L. Zhang, Y. Wu, Z. L. Wang, G. Zhu, *Adv. Mater.* **2017**, *29*, 1603115.

[5] a) Y. Q. Yang, N. Sun, Z. Wen, P. Cheng, H. C. Zheng, H. Y. Shao, Y. J. Xia, C. Chen, H. W. Lan, X. K. Xie, C. J. Zhou, J. Zhong, X. H. Sun, S. T. Lee, *ACS Nano* **2018**, *12*, 2027; b) H. Chu, H. Jang, Y. Lee, Y. Chae, J. H. Ahn, *Nano Energy* **2016**, *27*, 298; c) X. Pu, M. Liu, X. Chen, J. Sun, C. Du, Y. Zhang, J. Zhai, W. Hu, Z. L. Wang, *Sci. Adv.* **2017**, *3*, e1700015.

[6] B. Chen, W. Tang, T. Jiang, L. Zhu, X. Chen, C. He, L. Xu, H. Guo, P. Lin, D. Li, J. Shao, Z. L. Wang, *Nano Energy* **2018**, *45*, 380.

[7] S. Lambert, M. Wagner, *Chem. Soc. Rev.* **2017**, *46*, 6855.

[8] C. Minas, D. Carnelli, E. Tervoort, A. R. Studart, *Adv. Mater.* **2016**, *28*, 9993.

[9] R. Rai, M. Tallawi, A. Grigore, A. R. Boccaccini, *Prog. Polym. Sci.* **2012**, *37*, 1051.

[10] U. G. K. Wegst, M. F. Ashby, *Philos. Mag.* **2004**, *84*, 2167.

[11] F. Xing, Y. Jie, X. Cao, T. Li, N. Wang, *Nano Energy* **2017**, *42*, 138.

[12] T. Liu, Y. Inoue, K. Shibata, *Measurement* **2009**, *42*, 978.

[13] Y. D. Wang, Y. M. Kim, R. Langer, *J. Biol. Mater. Res. A* **2003**, *66A*, 192.

[14] Y. Wang, G. A. Ameer, B. J. Sheppard, R. Langer, *Nat. Biotechnol.* **2002**, *20*, 602.